JOURNAL OF CATALYSIS 117, 455–466 (1989)

Kinetic Implications of Mechanisms Proposed for Catalytic Carbon Filament Growth

E. C. BIANCHINI AND C. R. F. LUND[1]

Department of Chemical Engineering, State University of New York, Buffalo, New York 14260

Received November 7, 1988; revised January 31, 1989

The growth of carbon filaments from methane using an iron catalyst is studied. The dependence of the rate of reaction upon the gas phase composition, expressed as gas phase carbon activity, is observed to fall into two regimes. At low values of gas phase carbon activity the rate of reaction is linearly dependent upon this activity. At high values of gas phase carbon activity the rate of reaction is nearly independent of the gas phase composition. This behavior is observed over a range of temperatures which includes conditions under which both α-Fe^0 and γ-Fe^0 are thermodynamically favored. The results are interpreted in terms of mechanisms which have previously been suggested for this reaction. The results at high gas phase carbon activity are consistent with a mechanism where a thin surface carbide is present on the catalyst. The results at low gas phase carbon activity demonstrate that this mechanism cannot be valid under all conditions of filament growth. It is suggested that the gas phase equilibrates directly with the catalyst surface when the gas phase carbon activity is below the thermodynamic limit for the formation of the surface carbide. A mechanism by which catalyst deactivation proceeds is also proposed.

INTRODUCTION

The catalytic growth of carbon filaments has been studied for many years, and the subject of the mechanism of the reaction has been debated and refined since at least the early 1970s (*1–5*). It was accepted relatively early that a filament formed when carbon first deposited from the gas phase on one side of an active catalyst particle, then diffused through the catalyst particle bulk, and finally precipitated as a graphite-like structure at the other side of the catalyst particle (*3, 5–9*). The diffusion of carbon through the particle is generally accepted as the rate-determining step in this process. A concentration gradient from one side of the particle to the other will drive this diffusion step, and much of the early mechanistic study was directed at determining how this concentration gradient was established (thermal and "natural" means were proposed).

Thermal means of establishing the necessary gradient have received less attention recently, though Yang and Chen (*10*) have now suggested a means by which this mechanism can hold even during endothermic deposition reactions. The debate has shifted to the relative merit of different "natural" means by which it can be established. One important experimental observation is related to the conditions under which filament growth occurs. For a simple gas mixture like CO/CO_2 or CH_4/H_2 at fixed temperature and pressure the critical composition for carbon deposition can be calculated thermodynamically. A mixture with a greater CO or CH_4 content than that calculated would be predicted to lead to carbon deposition.

Rostrup-Nielsen (*4*) observed that carbon did not deposit when this critical composition was present and that in fact compositions which had slightly greater CO or CH_4 contents could be maintained without any carbon deposition occurring. This observation was explained by noting that the filaments are not pure graphite (which is the basis of the thermodynamic calculation of

[1] To whom correspondence should be addressed.

0021-9517/89 $3.00

the critical composition) and would be expected to have structural defects. Also, the surface energy of a filament would not be expected to be the same as that of pure graphite because the former is curved. Rostrup-Nielsen estimated the magnitude of these energy effects and showed that if the free energy change of the reaction was altered by such an amount, then the experimental observation could be rationalized in terms of thermodynamics.

Manning *et al.* (*11*) and Sacco and coworkers (*12–14*) made similar measurements and noted the same observations as Rostrup-Nielsen. They also noted, however, that the experimentally observed critical composition for filament growth nearly coincided with the critical composition calculated thermodynamically for the formation of θ-Fe_3C. Therefore they suggested that θ-Fe_3C was involved in the reaction mechanism, perhaps via some continuous formation and decomposition process.

In a similar series of experiments Geus and co-workers (*15–17*) measured experimentally the temperature dependence of the equilibrium constant for filament growth. The standard heat of reaction determined in this way was very nearly equal to the standard heat of formation of θ-Fe_3C, and it was *not* equal to the standard heat of reaction for carbon deposition as graphite. They also noted that the energy differences cited by Rostrup-Nielsen (i.e., crystalline imperfections and surface energy due to curvature) would be observed as changes in the standard heat of reaction, not as changes in the standard free energy change for the reaction. If they used the magnitudes which Rostrup-Nielsen had estimated for these effects to change the standard heat of reaction, the resultant value was still not equal to that which they had measured experimentally. On the basis of this observation and others discussed below they concluded that the active catalyst was a carbide.

Most recently, Alstrup (*18*) noted that there was another energy effect (in addition to the two factors which Rostrup-Nielsen had considered) which causes the energy of filaments to be different from that of pure graphite. This third effect is an elastic energy effect which Tibbets first used to explain the hollow nature of carbon filaments (*19*), and it arises from bending the basal planes of graphite. Alstrup showed that when all three terms were included, the change in the standard heat of reaction was large enough to yield the value which Geus and co-workers measured experimentally (*15*). This demonstrated that it was not *necessary* (though it was possible) that the catalyst be in carbide form when it was active.

Thus at present the thermodynamic observation of when carbon filaments can be formed is explained either if it is assumed that the catalyst must be a carbide or if it is assumed that the filaments are not graphite but instead differ energetically from graphite due to crystalline imperfections, surface energy effects, and elastic energy effects. There are other pertinent factors and observations which have led to two proposed mechanisms which will be considered in more detail now.

In addition to the thermodynamic study described previously (*15*), Geus and coworkers also performed catalyst characterization via magnetization methods and temperature-programmed hydrogenation (*16, 17*). The data were interpreted to indicate that a substoichiometric carbide (probably hexagonal) was the active phase. θ-Fe_3C was detected, but it was deemed to be an inactive side product. Geus and co-workers did not explain why the standard heat of reaction which they measured was equal to that of an inactive side product. The rate-determining step was still suggested to be the transport of carbon through the bulk of the catalyst. One feature which distinguishes the mechanism which they proposed is that the catalyst is a single phase whose composition varies from the side in contact with the gas to the side in contact with the filament. In terms of the schematic representation in Fig. 1a, the catalyst bulk

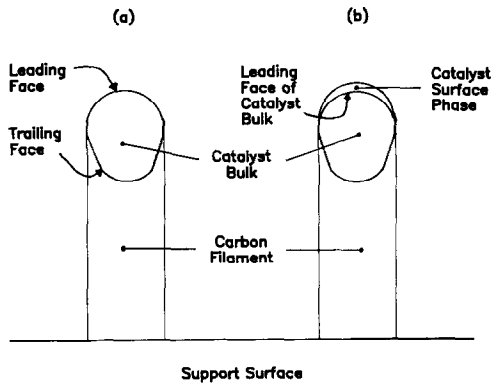

FIG. 1. Pictorial representation of the two variants of the catalyst morphology suggested in mechanisms proposed for the catalytic growth of carbon filaments. In variant (a) the catalyst particle is composed of a single phase throughout, whereas in variant (b) a very thin surface phase is present on the leading face of the catalyst separating the bulk of the catalyst from direct contact with the surrounding gas atmosphere.

is a single carbide phase, Fe_xC, where x is smaller at the leading face than at the trailing face.

Alstrup (*18*) considered studies with different metal crystal faces which showed different rates of carbon uptake, precipitation, and carbide formation. From these he arrived at a model which is represented schematically in Fig. 1b. The key feature of this model is that a surface carbide, only a few atomic layers thick, is proposed to form on the leading face of the catalyst. The rate-determining step is still the transport of carbon through the catalyst bulk, but the surface carbide fixes the carbon content at the leading face of the bulk of the catalyst. With this model Alstrup successfully explained the induction period which is observed experimentally before filament growth begins, the nonspherical shape of active catalyst particles, and the occurrence of octopus carbon. It should be noted that many features of this model are present in Sacco and co-workers' suggestion (*14, 20*) that diffusion of carbon through the metal was probably the rate-determining step in filament growth and that the mass flux was likely established due to the difference in solubility of carbon in the metal at the metal–metal carbide interface versus the metal–filament interface.

As already indicated, both these mechanisms can explain the thermodynamic observation of what conditions are necessary for filament growth. In this paper the kinetic implications of these two mechanisms are developed and compared to the results of experiments using an iron catalyst and CH_4/H_2 gas mixtures. The discussion will be developed in terms of the thermodynamic activity of carbon, a_C. Formally, a_C is the ratio of the fugacity of carbon as it exists in the reaction environment to the fugacity of carbon in its standard state (graphite) at the same temperature. In addition to being a convenient variable to use, this is in fact the proper variable to use in discussing the diffusion of carbon through a solid (*21*) (the rate-determining step in filament growth). It is, in fact, a gradient in the thermodynamic activity, not a gradient in concentration, which is the driving force for diffusion. (Darken has shown that carbon will diffuse from low concentration to high concentration if in so doing it can reduce its activity (*22*).)

Any CH_4/H_2 mixture can be characterized in terms of its gas phase carbon activity. First the equilibrium constant for reaction (1), K_1, must be calculated at the temperature of interest,

$$CH_4 \rightleftarrows C_{(\text{graphite})} + 2H_2. \qquad (1)$$

Then for any mixture of methane and hydrogen at that temperature the gas phase carbon activity is given by

$$a_C(\text{gas phase}) = \frac{K_1 \cdot P_{CH_4}}{(P_{H_2})^2} \qquad (2)$$

In addition, if any iron–carbon compound is formed, the gas phase activity of carbon necessary for formation of that compound can also be calculated. First the equilibrium constant for the formation of that compound from methane and iron at the temperature of interest is calculated. For exam-

ple, in the case of θ-Fe_3C the equilibrium constant, K_3, would be calculated for

$$3Fe + CH_4 \rightleftarrows \theta\text{-}Fe_3C + 2H_2. \quad (3)$$

The gas phase carbon activity necessary for formation of the compound is then equal to the ratio of that equilibrium constant to K_1; for example, the gas phase activity of carbon necessary to form θ-Fe_3C is given by

$$a_C(Fe_3C) = \frac{K_1}{K_3} \quad (4)$$

METHODS

The procedures and equipment used in this study are described in greater detail elsewhere (*23*). The catalyst used was iron; it was supported on L4100 powdered spectroscopic grade SP-1 graphite from Union Carbide. To prepare the catalyst the graphite powder was suspended in a solution formed by dissolving $Fe(NO_3)_2 \cdot 9H_2O$ (Aldrich reagent grade) in methanol (Fischer reagent grade). The solvent was evaporated at ca. 340 K over several hours and the resultant solid was lightly ground to break up aggregates of particles which formed during drying. The proportions of carbon and solution were chosen to produce a loading of 3.8 wt% iron.

The catalyst was pretreated in one of three ways, immediately before use. The simplest pretreatment was a low-temperature reduction (LTR) at 673 K in mixed flowing He [45 cm^3(stp) min^{-1}] and H_2 [7 cm^3(stp) min^{-1}] at ca. 100 kPa for 3 h. This was followed by evacuation at ca. 10^{-3} Pa for 30 min at the same temperature. Mössbauer spectroscopy using a sample treated in this way indicated the presence of only α-Fe^0.

The second pretreatment was a low-temperature carburization (LTC). The sample was first treated in He/H_2 as in the LTR only for 1 h instead of 3 h. The gas was then changed to flowing mixed He [60 cm^3(stp) min^{-1}], H_2 [20 cm^3(stp) min^{-1}], and CH_4 [20 cm^3(stp) min^{-1}] and the temperature was changed to 723 K. These conditions were maintained for 1 h. This was followed by evacuation at ca. 10^{-3} Pa for 30 min at the same temperature. The state of the catalyst after this treatment was also expected to be α-Fe^0.

The third pretreatment was a high-temperature carburization (HTC) and, like the LTR, it too began with treatment in He/H_2 only for 1 h instead of 3 h. The conditions were then switched to a $He/H_2/CH_4$ mixture as used in the LTC and the temperature was switched to 1123 K. These conditions were maintained for 1 h. This was followed by evacuation at ca. 10^{-3} Pa for 30 min at the same temperature. Mössbauer spectroscopy of a sample treated in this way indicated that about 20% of the sample was present as γ-Fe^0 after quenching to room temperature. It is expected that most if not all of the sample will be in the γ-Fe^0 state after the HTC pretreatment (i.e., without quenching).

The reactor system was all glass (quartz for the reactor, Pyrex elsewhere), and it operated in either flow mode or static recirculation mode. The catalyst was held in place between two quartz wool plugs in a horizontal reactor tube which was located inside an infrared furnace. Temperature was measured with a K-type thermocouple located in a thermocouple well which extended into the catalyst bed. Gas feed and vent lines could be closed off via stopcocks, leaving a loop which included a capacitance manometer, a magnetically driven recirculation pump, and the reactor (which could be bypassed). All volumes in the system were calibrated so that knowing the initial composition, the composition at any other time could be calculated by measuring the pressure versus time and assuming that only reaction (1) takes place. Mechanical and oil-diffusion pumps were also attached to the system for evacuation purposes.

Gases were fed from cylinders through rotameters where the flow rate was controlled. He (99.995%), CH_4 (99.97%), and H_2 (99.999%) were obtained from Linde.

He was further treated in a Suppelco carrier gas purifier. H_2 was further treated in sequential Oxiclear and Labclear purifiers. CH_4 was used as received.

Unless explicitly noted to the contrary, each experiment began by loading a fresh 1.25-g sample of catalyst into the reactor. After the reactor was checked for leaks one of the three pretreatments just described was effected. The temperature was adjusted to the desired reaction temperature with the sample still under vacuum. The reactor was then closed off and the remainder of the recirculation loop was charged with gas at whatever composition was desired. The recirculation pump was started (bypassing the reactor) and allowed to mix the gases for a few minutes. The reaction was started by closing the bypass loop and opening the flow through the reactor. The bed temperature and the pressure in the recirculation loop were recorded continuously on a strip chart recorder. The run ended by cooling to room temperature and rechecking for leaks.

A differential data analysis was used. The slopes of the traces recorded on the strip chart were measured at various times and converted into molar rates. The data were generally plotted as rate versus gas phase carbon activity. It should be noted that the gas phase carbon activity in the closed system begins at its highest value and decreases as reaction proceeds. Experimental tests and numerical calculations were performed, and they indicated that the measured rates are characteristic of a kinetic regime and that the recycle rate was great enough and the conversion per pass was small enough that the reactor could be modeled as a fully mixed batch reactor. Additionally, several runs reported in the next section were repeated, and it was observed that duplicate rates agreed to within 10%.

RESULTS

In two experiments graphite support material which had not been impregnated with iron catalyst was subjected to a LTR pretreatment. The reactor was then charged with pure methane at 27.8 and 28.7 kPa and exposed to reaction temperatures of 913 and 1033 K, respectively. A measurable rate of reaction, as indicated by an increase in pressure, was not observed at either temperature. Hence, in the absence of catalyst, the rate of deposition under the conditions of this study is negligible.

A fresh sample of Fe/graphite was subjected to a LTR pretreatment. The rate of reaction was then measured at 913 K and ca. 28.7 kPa (initial pressure) using pure methane. The results are presented (as circles) in Fig. 2 in the form of a plot of reaction rate versus gas phase carbon activity. At the end of the experimental run, the reactor was recharged with pure methane at the same temperature and pressure and the rate of reaction was again measured as a function of time. The results of this second run are also presented (as triangles) in Fig. 2. The lines in Fig. 2 are simply drawn as smooth curves through the data.

Another fresh sample of Fe/graphite was subjected to a HTC pretreatment. The rate of reaction at 1033 K was measured using pure methane initially at 28.4 kPa. The results are presented (as circles) in Fig. 3. At the end of the run the reactor was recharged with methane at 28.4 kPa and the

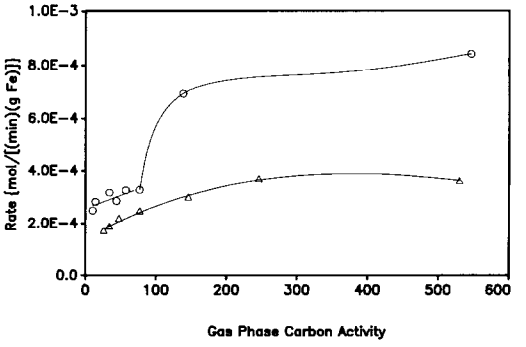

FIG. 2. Reaction rates observed after the low-temperature reduction pretreatment. The data represented by the circles are for a fresh catalyst sample; the data represented by the triangles are for the same sample in a repeat run.

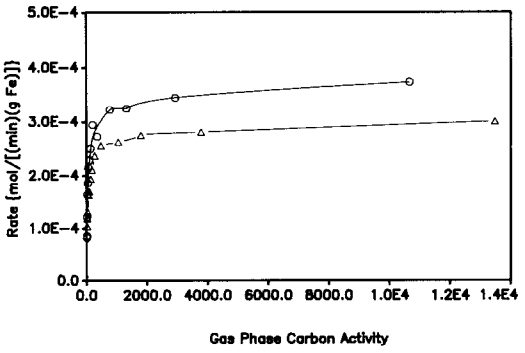

FIG. 3. Reaction rates observed after the high-temperature carburization pretreatment which is expected to yield a significant amount of γ-Fe^0. The data represented by the circles are for a fresh catalyst sample; the data represented by the triangles are for the same sample in a repeat run.

rate again measured at 1033 K. These results are presented (as triangles) in Fig. 3.

Three samples of fresh Fe/graphite were each subjected to a HTC pretreatment and subsequent rate measurement using pure methane initially at ca. 28.4 kPa. The temperature at which the rate was measured differed for each sample. The resulting data are plotted in Fig. 4. Similarly three fresh samples of Fe/graphite were each subjected to a LTC pretreatment and subsequent rate measurement using pure methane initially at ca. 28.4 kPa. Again the temperature at which the rate was measured differed for each sample, and the data are plotted in Fig. 5. In both these figures, the solid lines represent a least-squares, straight-line fit to the data. The line segment at low gas phase carbon activity was forced to pass through the point where rate equals zero when a_C = 1.0. The least-squares fitting used points below a_C = 10.0. In the high-a_C region, the fitting included all data where $a_C \geq 50.0$ (in the run at 913 K, the datum at a_C = 256 was not included in the fitting because the rate associated with this datum was higher than even the initial rate at a_C = infinity).

DISCUSSION

There are two important experimental phenomena suggested by an examination of Figs. 2 and 3. First, when a sample of Fe/graphite is used without a carburization pretreatment, an initial period of high reaction rate is observed. This can be seen in the first two data (i.e., the two points at the highest gas phase carbon activity) for the first run (circles) in Fig. 2. Similar behavior was exhibited by all samples given an LTR pretreatment. In the repeat run using the same catalyst (triangles, Fig. 2) this high reaction rate is not observed. Similarly, in the two back-to-back runs where the HTC pretreatment was used, Fig. 3, this high

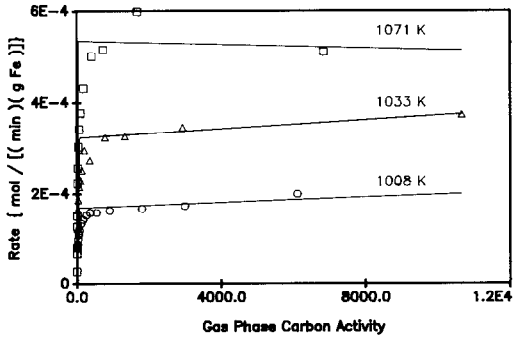

FIG. 4. Reaction rates measured as a function of gas phase carbon activity at three different temperatures. Each set of data represents a fresh catalyst sample which was pretreated by high-temperature carburization.

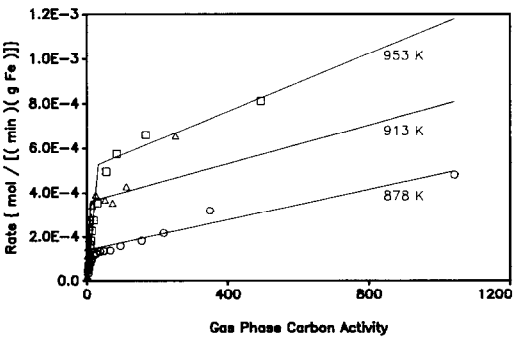

FIG. 5. Reaction rates measured as a function of gas phase carbon activity at three different temperatures. Each set of data represents a fresh catalyst sample which was pretreated by low-temperature carburization.

rate behavior is not observed. At present this phenomenon has not been studied in any greater depth. It is a transient event observed only with a fresh catalyst, and then only if the catalyst has not been precarburized. It also should be noted that the data in Fig. 2 for the initial run are after the induction period which many others have reported (i.e., the first datum represents the rate after 5 to 15 min of reaction).

The second phenomenon evident in both Figs. 2 and 3 is a continuous deactivation of the catalyst with time. In Fig. 3 it is shown that the rate under comparable conditions in a repeat run is lower than the rate under the same conditions in the first run. Deactivation is well known in the catalytic production of carbon filaments (*3–5, 22–25*). Transmission electron micrographs have shown evidence that as the reaction proceeds, some active particles become encapsulated in a graphitic carbon (*5*) and are thereby deactivated. Since the rates in the present study have been determined on the basis of catalyst mass, a steady decline in reaction rate would result from such a phenomenon, and this is what is believed to be responsible for the observed behavior. A comparison of Figs. 4 and 5 might then lead to the conclusion that deactivation is more rapid at lower temperatures; however, the pretreatments in these two figures are quite different. The HTR pretreatment certainly results in significant deactivation prior to the kinetic experiment and hence less during the run.

In both mechanisms described in the Introduction the rate-determining step is postulated to be the diffusion of carbon through the bulk of the catalyst. To rigorously model the rate of reaction by considering this step to be rate-determining, a catalyst particle like one of those shown in Fig. 1 should be chosen as the system, and the steady-state equation of continuity,

$$D \cdot \nabla^2(a_C) = 0, \qquad (5)$$

should be solved to give the carbon activity as a function of position within the particle. The different mechanistic models would require different boundary conditions and values for the diffusion coefficient, D. From the solution to Eq. (5), the flux of carbon across either the leading face or the trailing face could be evaluated.

For present purposes a much simplified model will be used. It will be assumed that there is an average diffusion path length, L, such that the carbon activity gradient from the front of the particle to the rear of the particle can be approximated as the difference between the activities at these two locations divided by the diffusion path length. In that case the rate of carbon diffusion can be represented by

$$r = D \cdot \frac{a_C(\text{leading face}) - a_C(\text{trailing face})}{L}. \qquad (6)$$

All steps prior to the diffusion of the carbon through the catalyst bulk may be assumed to be in pseudo-equilibrium.

The mechanism proposed by Alstrup (*18*) is applicable only above some minimum gas phase carbon activity, a_C^*. This must be so because the surface carbide he proposed is itself a phase, and consequently it will form only when thermodynamically favored. Alstrup suggests that the catalyst bulk is in fact θ-Fe_3C, so the surface carbide must be a higher carbide than this; he suggests either ε'-$Fe_{2.2}C$ or ε-Fe_2C. Hence, below a_C(surface carbide) the mechanism does not apply, and no speculation has been offered as to what will happen. Because all steps prior to the diffusion of carbon through the catalyst bulk may be assumed to be in pseudo-equilibrium, the activity of carbon in the bulk of the catalyst at leading face will be determined by pseudo-equilibrium with the surface carbide. In addition, since a nearly graphitic filament is precipitated at the trailing face, the activity of carbon in the bulk at the trailing face will be nearly equal to unity. Substitution in Eq. (6) indicates that the rate of reaction will then be given by

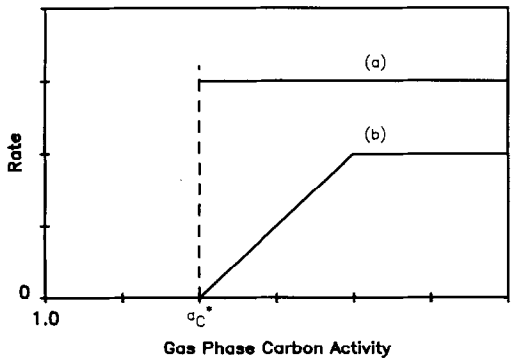

FIG. 6. Reaction rate behavior suggested by mechanisms which have been proposed: (a) the surface carbide mechanism, and (b) the hexagonal carbide of variable composition mechanism. In the latter case, other curve shapes might be possible (see Discussion).

$$r = D \cdot \frac{a_C(\text{surface carbide}) - 1.0}{L}. \quad (7)$$

This expression does not include any terms which depend upon the gas phase carbon activity (other than the fact that a minimum gas phase carbon activity which equals a_C(surface carbide) must be provided in order for the mechanism to hold). This behavior is indicated in curve a of Fig. 6.

Geus and co-workers (*15–17*) do not specify enough details to generate a specific dependence of the reaction rate upon activity. They do strongly suggest that the active phase is a hexagonal carbide, i.e., either ε'-$Fe_{2.2}C$ or ε-Fe_2C. In that case, the mechanism they propose would require that the rate be equal to zero for a_C(gas phase) < $a_C(\varepsilon'\text{-}Fe_{2.2}C)$, because this is the minimum condition for formation of the active phase. They then suggest that the gradient necessary for carbon diffusion is due to a variation in composition from the leading face of the catalyst to the trailing face. This might imply that further increasing the gas phase carbon activity would generate a more carbon-rich carbide at the leading face, at least until the gas phase carbon activity reached $a_C(\varepsilon\text{-}Fe_2C)$. This would generate the behavior represented by curve b in Fig. 6. The *shape* of this curve is speculation on the part of the present authors. However, for the mechanism proposed by this group to hold, it will be true that the activity will be zero below some minimum value and above this value the rate will initially increase with increasing gas phase carbon activity (i.e., as the carbide becomes able to attain a wider range of stoichiometry).

Neither of the curves presented in Fig. 6 matches the observed behavior shown in Figs. 4 and 5. The shape of curve b is similar to the experimental data, but it is shifted to higher values of a_C. At first glance the curve predicted by Alstrup's mechanism appears even further off. Alstrup's mechanism does not preclude catalytic activity below the critical a_C(surface carbide); it merely does not address this range of gas phase composition.

Clearly, if a_C(gas phase) < a_C(surface carbide) then the catalyst will appear as in Fig. 1a because the surface carbide cannot form thermodynamically. In this situation, returning to Eq. (6), a_C(leading face) is no longer fixed by a pseudo-equilibrium with the surface carbide. If, however, the diffusion step remains rate-determining then a_C(leading face) will still be fixed by a pseudo-equilibrium; in this case the pertinent steps in pseudo-equilibrium might be as given in

$$CH_4 + * \rightleftarrows CH_4 - * \quad (8)$$

$$CH_4 - * + * \rightleftarrows CH_3 - * + H - * \quad (9)$$

$$CH_3 - * + * \rightleftarrows CH_2 - * + H - * \quad (10)$$

$$CH_2 - * + * \rightleftarrows CH - * + H - * \quad (11)$$

$$CH - * + * \rightleftarrows C - * + H - * \quad (12)$$

$$2H - * \rightleftarrows 2* + H_2 \quad (13)$$

$$C - * \rightleftarrows * + C_{\text{dissolved at leading face}} \quad (14)$$

The equilibrium expressions for this group of reactions can be solved and combined with Eq. (2) to show that the carbon activity at the leading face is given by

$$a_C(\text{leading face}) = K \cdot a_C(\text{gas phase}). \quad (15)$$

Again the carbon activity at the trailing face will be determined by the precipitation of the filamentous carbon with $a_C \simeq 1.0$; substitution in Eq. (6) gives the predicted dependence of the rate on the gas phase activity,

$$r = D \cdot \frac{K \cdot a_C(\text{gas phase}) - 1.0}{L}. \quad (16)$$

As can be seen from Eq. (16), the rate of reaction is predicted to be linearly proportional to the gas phase carbon activity in this region. The combined behavior using Alstrup's model for $a_C > a_C$(surface carbide) and the relationship developed above for $a_C < a_C$(surface carbide) is represented in Fig. 7.

The behavior depicted in Fig. 7 looks very much like that seen in Figs. 4 and 5. This is even more evident when the low a_C region of one of the lower temperature curves from Fig. 5 is expanded as shown in Fig. 8. In fact there is only one significant difference between the observed behavior and that predicted from the mechanistic considerations, namely that at high a_C the mechanisms predict no dependence of the rate upon the gas phase carbon activity whereas the experimental data suggest a very weak dependence. In fact what appears to be a very weak dependence of the rate upon the gas phase carbon activity is more likely due to the steady deactivation

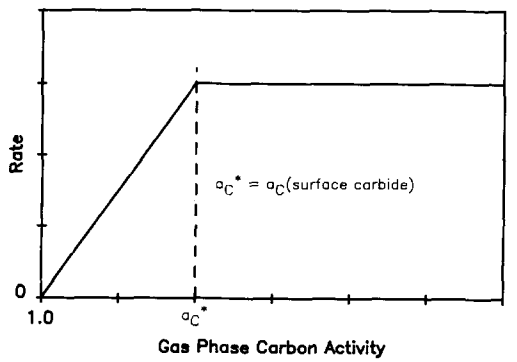

FIG. 7. Reaction rate behavior suggested by extension of the surface carbide mechanism.

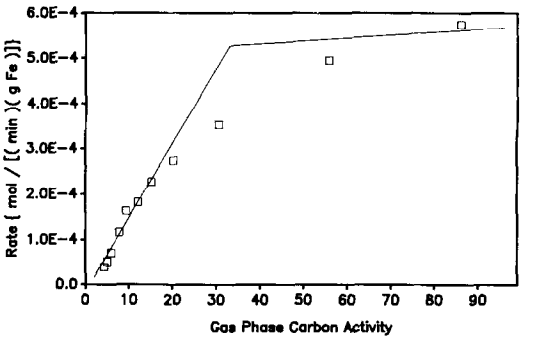

FIG. 8. Reaction rate behavior in the low gas phase carbon activity region for the experiment at 953 K shown in Fig. 5. The two lines represent least-square fits to the data, and that at higher a_C was fit primarily with data which lie off scale.

of the catalyst with time which was mentioned at the beginning of this section. It is possible to estimate the rate of catalyst deactivation from the data presented in Figs. 1 and 2, and when this is done it fully supports the contention that the apparent dependence of reaction rate upon gas phase carbon activity at high values of a_C suggested in Figs. 4 and 5 is primarily due to catalyst deactivation.

This is not the first report of a linear dependence of the rate upon a_C(gas phase) at low values of the latter quantity. Audier and co-workers (*26–29*) observed virtually identical behavior using iron–nickel and iron–cobalt catalysts with both CO/CO_2 and CH_4/H_2. In fact, the rates measured in the present work are equal within experimental error to those reported for iron–nickel (*29*). However, in that work a_C(gas phase) never exceeded approximately 16, and consequently the region where the rate does not depend upon a_C(gas phase) was never observed.

This mechanistic picture, which is consistent with the kinetic data, suggests at least two consequences. First, it is possible in principle to identify which carbide is the surface carbide by noting the value of a_C where the rate first becomes independent of the gas phase carbon activity. This value of

a_C should equal the activity of carbon in the surface carbide. For the experiments in Fig. 5 this value is in the range 15 to 25. Unfortunately, thermodynamic data for any of the carbides other than θ-Fe_3C and some limited data for χ-Fe_5C_2 have not been located, and consequently the identification of the surface carbide has been hindered.

Additionally the mechanism suggests that the temperature dependence of the rate of reaction at fixed gas composition and pressure may be different in the low-a_C region from that in the high-a_C region. This is most clearly seen from Eqs. (7) and (16). Considering first the low-a_C region, there are two terms in Eq. (16) which will have a temperature dependence, namely D and K. Both of these quantities will vary exponentially with the reciprocal of the absolute temperature. Furthermore, the rate expression consists of two terms, one containing only D and the other containing both D and K. It would be pure speculation to predict which term will dominate. No attempt was made to determine an apparent activation energy in this region. This is because the catalysts in the present study were observed to be undergoing deactivation, and the deactivation would be expected to occur at different rates at different temperatures. Also, the region of low a_C was not reached until some time into the experiments, and this length of time was different for runs at different temperatures.

Apparent activation energies were determined from *initial* rate data for three sets of samples: one with each of the three pretreatments. These activation energies were determined from runs at three temperatures, namely from the initial rate data measured in Figs. 4 and 5 along with a set of measurements under conditions analogous to those in Fig. 5 only where an LTC pretreatment was used. Equation (7) also includes two terms which can contribute to the temperature dependence: D again and a_C(surface carbide). It may be expected, however, that the temperature dependence of the latter will be quite small compared to the dependence of D. For example, $a_C(\theta$-$Fe_3C)$ varies from 1.79 to 0.95 as the temperature varies from 878 to 1071 K. Thus it is expected that the temperature dependence of the rate of reaction will essentially equal that of the diffusion coefficient of carbon in the catalyst.

The initial rates from the high-temperature series of runs shown in Fig. 4 are consistent with this expectation. In this temperature and composition range γ-Fe^0 is expected to be the thermodynamically stable phase, and the apparent activation energy calculated from these runs is 145.2 ± 15 kJ/mol. This compares well with the value measured via controlled atmosphere electron microscopy (CAEM) (*30*), 141.8 kJ/mol, when the catalyst was γ-Fe^0, as well as with values reported for the activation energy of D for γ-Fe^0: 146 kJ/mol (*31*), 150.2 kJ/mol (*32*), and 131.2 to 150.6 kJ/mol (*21*). The initial rates from experiments where the LTR and LTC pretreatments were used yielded activation energies with high uncertainties (only three temperatures were studied).

The kinetic data for the higher temperatures experiments (i.e., γ-Fe^0) do not yield a sharp break at some critical a_C^*. Instead, there is a smooth transition from high dependence of the rate upon gas phase carbon activity to low dependence as the gas phase carbon activity increases. At present it is not clear whether this is because the modified form of Alstrup's mechanism does not apply to γ-Fe^0 (*24*) or because of deactivation problems associated with the high reaction temperatures.

To summarize, in the present work the dependence of the rate of filament production upon a_C(gas phase) has been studied. At low a_C the rate was observed to depend linearly upon a_C as Audier and Coulon (*29*) had previously reported. However, above a certain critical a_C the rate became essentially independent of a_C. This behavior is shown most clearly in Fig. 8. This behavior can be explained in mechanistic terms by considering the catalyst to be a single phase

throughout at low a_C as shown in Fig. 1a. In this situation the gas phase equilibrates directly with the catalyst surface at the leading face through a series of steps such as given in reactions (8) through (14). This leads to a rate expression, Eq. (16), which shows a linear dependence of the rate upon a_C(gas phase). The critical a_C is simply the thermodynamic limit at which a surface carbide is allowed to form, and this results in a transformation of the catalyst to the morphology depicted in Fig. 1b which was suggested by Alstrup. At this point the rate becomes independent of a_C(gas phase) as indicated by the rate expression, Eq. (7).

It is interesting to speculate about the deactivation of the catalyst in terms of the Alstrup mechanism as it has been extended in the present work. Alstrup postulated that the surface carbide was very thin. Perhaps instead the surface carbide is a phase which grows very slowly and in fact it is increasing in thickness as the reaction proceeds. Deactivation of the catalyst then might occur when the surface carbide reached some critical thickness. At that point it could then decompose into graphite and a lower carbide. The graphite would precipitate at the surface thereby blocking the gas phase from contact with the catalyst, and at that point the particle would be deactivated. The carbon remaining in the particle would then redistribute uniformly throughout the particle. This might result in a transformation of the entire particle into θ-Fe_3C and would explain the large amounts of this material which have been observed after filament growth. This would suggest that catalyst deactivation could be avoided and longer filaments could be produced if the reaction environment were controlled so that operation takes place in the low-a_C region where the rate is proportional to the gas phase carbon activity. In this region the surface carbide cannot form; hence it could not grow and eventually decompose producing the graphite which would deactivate the catalyst. We anticipate testing this speculation in the near future.

ACKNOWLEDGMENTS

This material is based upon work supported by the National Science Foundation under Grant MSM-8707606. One of the authors (E.C.B.) thanks the Center for Integrated Process Systems Technology at the State University of New York at Buffalo for support during the performance of this work.

REFERENCES

1. Ruston, W. R., Warzee, M., Hennaut, J., and Waty, J., *Carbon* **7,** 47 (1969).
2. Robertson, S. D., *Carbon* **8,** 365 (1970).
3. Baker, R. T. K., Barber, M. A., Feates, F. S., Harris, P. S., and Waite, R. J., *J. Catal.* **26,** 51 (1972).
4. Rostrup-Nielsen, J. R., *J. Catal.* **27,** 343 (1972).
5. Baker, R. T. K., Harris, P. S., Thomas, R. B., and Waite, R. J., *J. Catal.* **30,** 86 (1973).
6. Lobo, L. S., Trimm, D. L., and Figueiredo, J. L., *in* "Proceedings, 5th International Congress on Catalysis, Palm Beach, 1972" (J. W. Hightower, Ed.). North-Holland, Amsterdam, 1973.
7. Lobo, L. S., and Trimm, D. L., *J. Catal.* **29,** 15 (1973).
8. Bernardo, C. A., and Lobo, L. S., *J. Catal.* **37,** 267 (1975).
9. Rostrup-Nielsen, J. R., and Trimm, D. L., *J. Catal.* **48,** 155 (1977).
10. Yang, R. T., and Chen, J. P., *J. Catal.* **115,** 52 (1989).
11. Manning, M. P., Garmirian, J. E., and Reid, R. C., *Ind. Eng. Chem. Process Des. Dev.* **21,** 404 (1982).
12. Sacco, A., Jr., and Reid, R. C., *AIChE J.* **25,** 839 (1979).
13. Sacco, A., Jr., and Caulmare, J. C., *ACS Symp. Ser.* **202,** 177 (1982).
14. Sacco, A., Jr., Thacker, P., Chang, T. N., and Chiang, A. T. S., *J. Catal.* **85,** 224 (1984).
15. deBokx, P. K., Kock, A. J. H. M., Boellaard, E., Klop, W., and Geus, J. W., *J. Catal.* **96,** 454 (1985).
16. Kock, A. J. H. M., deBokx, P. K., Boellaard, E., Klop, W., and Geus, J. W., *J. Catal.* **96,** 468 (1985).
17. Boellaard, E., deBokx, P. K., Kock, A. J. H. M., and Geus, J. W., *J. Catal.* **96,** 481 (1985).
18. Alstrup, I., *J. Catal.* **109,** 241 (1988).
19. Tibbetts, G. G., *J. Cryst. Growth* **66,** 632 (1984).
20. Sacco, A., Jr., and Thacker, P., *in* "Ext. Abstr. Prog., 16th Bienn. Conf. Carbon, Univ. Calif., San Diego, July 18–25, 1983," p. 525.
21. Kristal, M. A., *in* "Diffusion Processes in Iron Alloys" (R. Wald, Transl., and J. J. Becker, Ed.). Israel Program for Scientific Translation, Jerusalem, 1970.

22. Darken, L. S., *Trans. AIME* **180,** 430 (1949).
23. Bianchini, E., M. S. thesis, SUNY at Buffalo, 1988.
24. Tibbetts, G. G., Devour, M. G., and Rodda, E. J., *Carbon* **25,** 367 (1987).
25. Cooper, B. J., and Trimm, D. L., *J. Catal.* **62,** 35 (1980).
26. Audier, M., Coulon, M., and Bonnetain, L., *Carbon* **21,** 93 (1983).
27. Audier, M., Coulon, M., and Bonnetain, L., *Carbon* **21,** 99 (1983).
28. Audier, M., Coulon, M., and Bonnetain, L., *Carbon* **21,** 105 (1983).
29. Audier, M., and Coulon, M., *Carbon* **23,** 317 (1985).
30. Baker, R. T. K., Chludzinski, J. J., Jr., and Lund, C. R. F., *Carbon* **25,** 295 (1987).
31. Birks, N., and Nicholson, A., *in* "Proceedings, Mathematical Models in Metallurgical Process Development." ISI Publication No. 123, Iron and Steel Institute, London, 1970.
32. Tricot, R., and Castro, R., "The Metallurgical Evolution of Stainless Steels" (F. B. Pickering, Ed.). American Society for Metals, Metals Park, OH 1966; Wells, C., Batz, W., and Mehl, R., *Trans. AIME* **188,** 553 (1950).